Incomplete sensitivities in design and control of fluidic channels

By B. Mohammadi, R. Bharadwaj, J. I. Molho AND J. G. Santiago

1. Motivation and objectives

Control of distributed systems has various industrial applications, as it is often desired to keep complex multi-disciplinary systems in some given state. Definition or parameterization of control space is the first main issue we face when formulating a control problem. Usually, one wishes to keep the parameterization space dimension as small as possible to limit the complexity of the problem. In addition, for any control approach to be effective, it should be realizable during the time the system is still controllable. Computational cost is therefore another critical issue. Our aim in this paper is to discuss alternative remedies for these two problems. We discuss the behavior of an electrokinetic microchannel system where the control variables include both the geometry of the microchannels and the temporal control of potentials. In a real system, the geometric control is achieved by the realization of etched microchannel structures using microlithography techniques. Flow control is accomplished by applying electric potentials along microchannels. We discuss the behavior of our design and control platform for two complementary classes of problems: the situation where the number of controls is small (a potential field) and where the number of controls is large (the geometry of a microchannel turn).

We use our sub-optimal control technique, using accurate gradient evaluation, for the first class of problems. For second class, we show that the sub-optimal control is also efficient using incomplete evaluation of the gradient, but only for a limited class of cost functions. Our motivation here comes from the fact that, for a control algorithm based on gradient methods to be efficient, the design should have the same complexity as the direct problem. We therefore need a cheap and easy gradient evaluation somehow avoiding the adjoint equation solution.

Since the problem involves electrostactics, electromigration, and fluid motion, we couple several differential state equations in the simulation. In that context, the gradient-based minimization algorithm is reformulated as a dynamic system, which is considered as an extra state equation for the parameterization. This formulation makes it easier to understand the coupling between different components of the simulation. We look for the solutions to our optimization problem as stationary solutions of a second order dynamic system. In addition, for the system to have global search features, we use the natural instability of second order hyperbolic systems (Attouch & Cominetti 1996).

2. Dynamic shape optimization and state control

Consider the following optimization or control problem:

$$\min_{x(t)} J(x(t), q(x), U(q), \nabla U(q)), \tag{2.1}$$

$$E(x(t), q(x), U(q), \nabla U(q)) = 0,$$

$$g_1(x(t)) \leq 0, g_2(q) \leq 0, g_3(q, U(q)) \leq 0,$$

where J is the cost function, $x \in R^n$ describes the parameterization, q describes geometrical entities (normals, surfaces, volumes,...), $U \in R^N$ denotes the state variables, $E \in R^N$ is the time dependent state equations, g_1 defines the constraints on the parameterization, g_2 those on geometrical quantities and g_3 defines the state constraints. Details of the definition of the control and design configurations are given by Mohammadi & Santiago (2001).

2.1. *State equations*

The problem of interest here concerns separation of charged species in an aqueous electrolyte solution by application of an electric field. The driving force for separation is the differences in electrophoretic mobilities (Probstein 1995).

The electric field $E = -\nabla\phi$ (V/m) is the solution of the following Poisson-Boltzmann equation for the potential ϕ:

$$\nabla.E = -\Delta\phi = \frac{1}{\epsilon_r\epsilon_0}\rho_e, \quad \text{in } \Omega \tag{2.2}$$

$$\phi(\Gamma_{in}) = v_1, \quad \phi(\Gamma_{out}) = v_2,$$

$$\phi = \phi_3 \quad \text{or} \quad \frac{\partial\phi}{\partial n} = 0 \quad \text{on other boundaries.}$$

where $\rho_e = \sum_{i=1}^{n} F z_i C_i$ is the net charge density (Coulomb/m^3), $z_i \in \mathbf{Z}$ is the valence number for the species i of molar concentration C_i (mol/m^3). F is the Faraday constant ($F = 96500$) and ϵ_r and ϵ_o are the permittivity constants (respectively the relative and free space permittivities). The dielectric constant $\epsilon_r\epsilon_0 \sim 10^{-9}$. It is important to notice that for most applications, the net charge density is nearly zero in the bulk.

The flow velocity is described by the Navier-Stokes equation with Lorentz forces:

$$\rho\frac{\partial U}{\partial t} - \mu\Delta U + \nabla p = \rho_e\nabla\phi, \quad \text{in the channel} \tag{2.3}$$

$$U = 0 \quad \text{on channel walls,}$$

$$-\mu\frac{\partial U}{\partial n} + p.n = 0 \quad \text{in and outflow boundaries.}$$

One difficulty in simulating electroosmotic flows is the computation of the velocity field in the electrical double layer(EDL). EDL refers to the interfacial region between the wall and the bulk solution, where ions having charge opposite to that of the channel wall, accumulate when the wall is brought into contact with the solution. The thickness of the EDL, at typical salt concentrations, is a few nanometers. Thus a very fine mesh near the channel surface is needed to describe the flow in the EDL. To avoid this computationally expensive step, the classical no-slip condition at the wall can be replaced by defining a shear plane near the wall. The velocity at the shear plane is given by the Smoluchowski equation:

$$U = \frac{-\epsilon_0\epsilon_r E\zeta}{\mu}, \tag{2.4}$$

where μ is the dynamical viscosity (Kg/(m s)), ρ the flow density (Kg/m^3), p the pressure (Pascal) and U the flow velocity (m/s).

$\zeta(C_i)$, called the zeta potential, is the potential at the slip plane. Zeta potential is a function of the surface charge density and the local species concentration.

The species are advected using the following advection-diffusion-reaction equations:

$$\frac{\partial C_i}{\partial t} = -\nabla.j_i, \tag{2.5}$$

where

$$j_i = -\nu_i z_i F C_i \nabla\phi - D_i \nabla C_i + C_i U + R_i(C), \tag{2.6}$$

where ν_i is the electrophoretic mobility, D_i is the diffusivity and R_i is the rate of reaction for species i.

An equation for the generation of charge density can be derived by summation over the species conservation equations:

$$\frac{\partial \rho_e}{\partial t} = -\nabla.i = 0, \tag{2.7}$$

where i is the current charge density:

$$i = F \sum_{i=1}^{n} z_i j_i,$$

where j_i is given by Eq. (**??**). In addition, we have $\sum_i R_i = 0$.

Away from the EDL, aqueous electrolyte solutions have negligible net charge density (i.e. $\rho_e = 0$). For such a case, the above equations yield a new equation for the potential ϕ instead of the Poisson-Boltzmann equation:

$$-F\nabla.((\sum_{i=1}^{n} \nu_i z_i C_i)\nabla\phi) = \nabla.(\sum_{i=1}^{n} D_i z_i \nabla C_i). \tag{2.8}$$

This ensemble of governing equations is quite complex and it would be preferable not to use the above set of equations for sensitivity evaluation. This is the motivation behind using incomplete sensitivities presented below (Mohammadi & Pironneau 2001).

2.2. *Closure equation for $x(t)$*

In our approach, minimization algorithms are seen as closure equations for the parameterization. In other words, we introduce a new time-dependent problem for $x(t)$. This can also be seen as an equation for the structure. We can show that most linear or quadratic gradient-based minimization algorithms can be expressed in the following form:

$$-\dot{x} + \epsilon \ \ddot{x} = F(\Pi, M^{-1}, (\nabla_{xx} J)^{-1}, \nabla_x J), \tag{2.9}$$

where F is a function of the exact or incomplete gradient and of the inverse of the Hessian of the cost function. It also takes into account the projection over the admissible space Π and the smoothing operator we use when using the CAD-free parameterization (Mohammadi & Pironneau 2001). Usually, Π does not depend on p except when using mesh adaptation.

Let us consider the particular case of $\epsilon > 0$, where we recover the so called heavy ball method (Attouch & Cominetti 1996; Cabot 2001 and Mohammadi 1999b). The aim of this approach is to access different minima of the problem, and not only the nearest local minimum, by facilitating escape from the local minima by introduction of second-order perturbation terms. The difference with the original heavy-ball method is that here the method is seen as a perturbation of the first-order derivative while in the original method the steepest descent is seen as a perturbation of the hyperbolic second-order system.

This reformulation is suitable for numerical experiments as it enables us to tune the perturbation to be as small as possible. This is especially true for complex applications (e.g., with coupled physics), as the optimization process otherwise becomes difficult.

Another interesting feature of the dynamic minimization algorithm is a possible coupling between several balls (points in the admissible control space) to improve the global search ability by communicating information between balls on their respective state. The idea is therefore to solve the pseudo-unsteady system (Mohammadi 1999b) from different ball positions and to couple the paths using exchange of information about global gradients (Cabot 2001). Consider, q balls $x_j, j = 1, .., q$, following the motion prescribed by q pseudo-unsteady systems:

$$-\dot{x_j} + \epsilon \;\; \ddot{x_j} = -(F_j + G_j), \tag{2.10}$$

where F_j is as in Eq. (**??**) and G_j a global gradient representing the interaction between balls (recall that each ball is a design configuration). To reach the global minima, the number of balls has to be large enough. A good estimate for this number is given by the dimension of the design space (n). Even with this number the complexity is negligible compared to that of evolutionary algorithms. Our experience shows that the following choice of G_j is satisfactory(see example below):

$$(G_j)_i = \sum_{k=1,k\neq j}^{q} \frac{J_j - J_k}{||x_j - x_k||^2}(x_{j_i} - x_{ki}), \quad \text{for} \quad j = 1, .., q, \quad i = 1, .., n. \tag{2.11}$$

However, in CAD-free parameterization, n can be quite large and, due to the required computational effort for one simulation, we cannot afford more than a few (say 3 or 4) shape evolutions at the same time. This approach can therefore be seen as an improvement over the search capacity of the original algorithm. In addition, the process is suitable for a distributed treatment as in evolutionary-type minimizations.

We show below the behavior of the pseudo-unsteady systems with two balls and constant λ and ϵ for the minimization of a function having several local minima (the global minimum is reached at (0,0)). For $(x, y) \in]-10, 10[\times]-10, 10[$ consider J defined by:

$$J(x, y) = 1 - \cos(x)\cos(\frac{y}{\sqrt{2}}) + \frac{1}{50}((x - y/2)^2 + 1.75y^2). \tag{2.12}$$

The aim is to show that the heavy-ball method improves a global-minimum search by facilitating escape from the local minima. However, finding the global minima requires several trials, but coupling several heavy balls can help in finding the global minima, even though individual balls may not converge to the global minima.

3. Sensitivities and incomplete sensitivities

Consider the following general simulation loop:

$$J(x) : x \to q(x) \to U(q(x)) \to J(x, q(x), U(q(x))).$$

The gradient of J with respect to x is:

$$\frac{dJ}{dx} = \frac{\partial J}{\partial x} + \frac{\partial J}{\partial q}\frac{\partial q}{\partial x} + \frac{\partial J}{\partial U}\frac{\partial U}{\partial q}\frac{\partial q}{\partial x}. \tag{3.1}$$

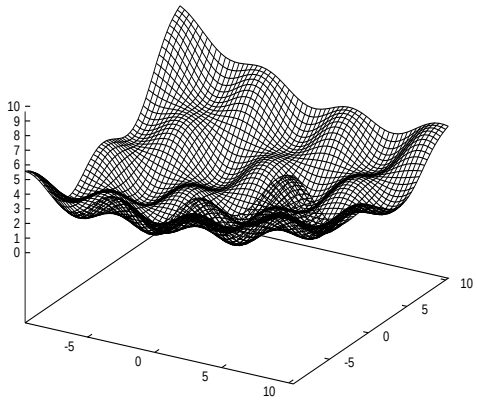

FIGURE 1. Graph of $J(x, y)$ given by **??**.

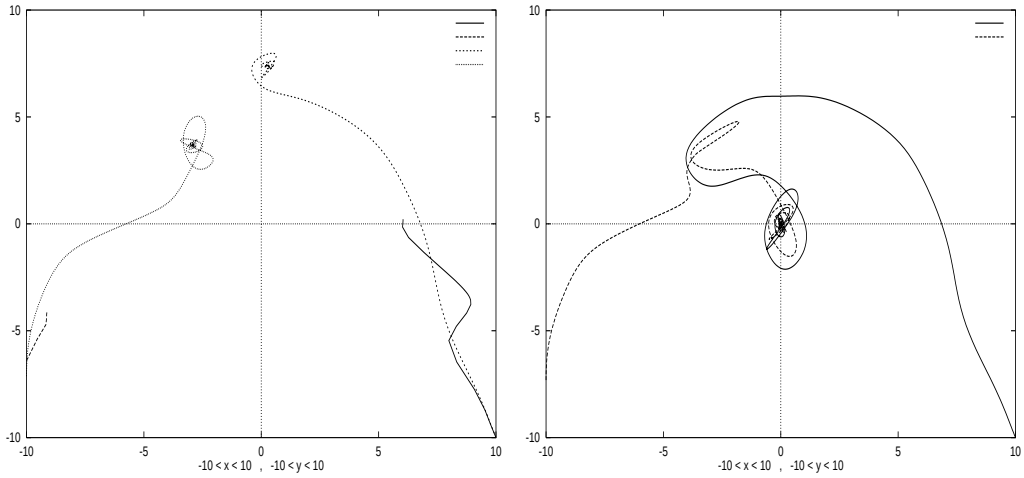

FIGURE 2. Left: Paths for the steepest-descent and heavy-ball methods starting from two different points. Right: By coupling the two balls in the heavy-ball method using the global gradient, the global minimum is reached.

If the following requirements hold, we can introduce incomplete evaluation of this gradient, reducing the computational cost:

- If both the cost function and control space are defined on the shape (or on some part of it),
- if J is of the form

$$J(x) = \int_{\text{shape}} f(x)g(u)d\gamma,$$

- and if the local curvature of the shape is not too large.

The incomplete-sensitivity approach means that we can drop the last term in Eq. (**??**). This does not mean, as seen below, that a precise evaluation of the state is unnecessary,

but that for a small change in the shape the state will remain almost unchanged, while geometrical quantities have variations of the same order as for the shape.

3.1. *Illustration of a few simple examples*

The argument behind incomplete sensitivities has already been successfully used in the so called classical equivalent-injection boundary conditions. These conditions are designed to study the effect of small deformations to the shape without actually analyzing deformations. Recall the implicit relation for the slip velocity on a fixed shape (subscript f) reproducing its displacement (subscript m). If we suppose that $u_m \sim u_f$, which means that the sensitivity with respect to the shape dominates, we have (Mohammadi 1999a):

$$u_f.n_f = -u_f(n_m - n_f) + V.n_m, \tag{3.2}$$

where V is the speed of the moving shape in the fixed frame attached to the fixed shape. In the same way, sensitivity analysis for the product $u.n$ with respect to the shape x gives:

$$\frac{d}{dx}(u.n) = \frac{\partial u}{\partial x}.n + u\frac{\partial n}{\partial x} \sim u\frac{\partial n}{\partial x}, \tag{3.3}$$

where as for the transpiration condition above we supposed that $\frac{\partial u}{\partial x} << \frac{\partial n}{\partial x}$. We see that the state has to be accurate, and that it is more important to have an exact state evaluation and an approximate gradient rather than a precise (in term of operators accounted in the linearization) gradient evaluation based on a wrong state. This point is critical as designers are penalized by the cost of sensitivity evaluations which frequently drives them to use coarser meshes in the optimization than the meshes they normally use for simulations without optimization.

Consider as cost function $J = au_x(a)$ and as state equation the following steady advection-diffusion equation:

$$u_x - Pe^{-1}\ u_{xx} = 0,$$
$$\text{on } \ ]a,1[, \quad u(a) = 0, \quad u(1) = 1. \tag{3.4}$$

The solution of this equation is:

$$u(x) \ = \ \frac{\exp(Pe^{-1}\ a) - \exp(Pe^{-1}\ x)}{\exp(Pe^{-1}\ a) - \exp(Pe^{-1})}. \tag{3.5}$$

We are looking for $J_a(a) = u_x(a) + a(u_x)_a(a)$. We are in the domain of applicability of the incomplete sensitivities, where the cost function involves products of state and geometrical quantities and is defined at the boundary:

$$J_a(a) = u_x\ (a)(1 + a\frac{Pe^{-1}\ \exp(Pe^{-1}\ a)}{\exp(Pe^{-1}\ a) - \exp(Pe^{-1})}). \tag{3.6}$$

The second term in the parenthesis is the state-linearization contribution which is negligible for large Peclet number. In all cases, the sign of the sensitivity is always correct.

The analysis also holds for nonlinear PDEs such as the Burgers equation. Indeed, consider as cost function $J(a) = au_x(a)$ and as state the steady solution of the Burgers equation

seen before, a being the left boundary location:

$$u_t + 0.5(u^2)_x = 0.3xu, \quad \text{on} \quad]a,1[, \quad u(a) = 1, \quad u(1) = -0.8. \tag{3.7}$$

We have $J_a(a) = u_x(a) + a(u_x)_a(a)$. We are in the domain of applicability of incomplete sensitivities. In view of the Burgers equation, we have $u_x(a) = 0.3\,a$ and the exact gradient ($J_a(a) = 0.3a + 0.3a$) can be compared to the incomplete one ($0.3a$). We can see again that the sign of the gradient is correct (as is always the case) and there is only a factor of 2 between the exact and incomplete gradients.

Another example concerns the sensitivity analysis for the flow rate of a Poiseuille flow in a channel driven by a constant pressure gradient (p_x) with respect to the channel width. The walls are at $y = +/-a$. The flow velocity satisfies:

$$u_{yy} = \frac{p_x}{\nu}, \quad u(-a) = u(a) = 0. \tag{3.8}$$

The analytical solution satisfying the boundary conditions is: $u(a,y) = \frac{p_x}{2\nu}(y^2 - a^2)$.

The flow rate is given by $J(a) = \int_{-a}^{a} u(a,y)dy \quad (= \frac{-2p_x a^3}{3\nu})$. The gradient is given by (using the boundary conditions in Eq. (**??**)):

$$\frac{dJ}{da} = \int_{-a}^{a} \partial_a U(a,y)dy = \frac{-2a^2 p_x}{\nu}, \tag{3.9}$$

while the incomplete sensitivity vanishes. Indeed, in this example we are not in the (Mohammadi & Pironneau 2001) domain of applicability of sensitivity analysis because the cost fnction is not a product of the state and geometrical entities.

Now consider the following cost function obtained by multiplying the flow rate by a: $\tilde{J}(a,u) = \int_{-a}^{a} au(a,y)dy$, which has sensitivity given by:

$$\frac{d\tilde{J}}{da} = J + a\frac{dJ}{da} = \frac{-p_x a^3}{\nu}(\frac{2}{3} + 2), \tag{3.10}$$

and here the incomplete sensitivity is $\frac{-2p_x a^3}{3\nu}$. This quantity always has the right sign and is a good example of how to reduce the cost of sensitivity evaluation by an appropriate redefinition of cost function.

4. Reduced complexity models and incomplete sensitivities

As described earlier, we drop the sensitivity with respect to the state in incomplete sensitivities. One way to improve this approximation cheaply is to use reduced models to provide these sensitivities. In other words, consider the following reduced model for the definition of $\tilde{U} \sim U$:

$$x \to q(x) \to \tilde{U}(q(x))(\frac{U}{\tilde{U}}),$$

where $\tilde{U}$ is the solution of a reduced low-complexity model (wall functions, for instance). The last term is an identification term for the reduced model, to produce the same results as the full state equation.

The incomplete gradient of J with respect to x can be improved by adding the last

part from the exact gradient, but computed based on this model:

$$\frac{dJ}{dx} \sim \frac{\partial J(U)}{\partial x} + \frac{\partial J(U)}{\partial q}\frac{\partial q}{\partial x} + \frac{\partial J(U)}{\partial U}\frac{\partial \tilde{U}}{\partial q}\frac{\partial q}{\partial x}\frac{U}{\tilde{U}}. \tag{4.1}$$

We can see that $\tilde{U}$ is never used, only $\partial\tilde{U}/\partial q$. It is also important to notice that the reduced models need to be valid only over the support of the control parameters. We see below an example of such simplification.

5. Cost function and its redefinition

The original cost function we consider is designed to minimize the skew and band dispersion for the advected species and uses the fact that the iso-contours of an advected specie C need to remain normal to the flow velocity:

$$J(x) = \int_{\omega} (\nabla C \times U(\alpha))^2 dx. \tag{5.1}$$

We see that we are not in the admissibility domain of incomplete sensitivities becasue the cost function is defined over the whole channel.

To be suitable for incomplete sensitivities, we introduce the following approximate cost function, based on migration time along the walls of the channel to minimize the skew:

$$\begin{aligned} J(x) = (\int_{\Gamma_i} \frac{ds}{U.\vec{\tau}} - \int_{\Gamma_o} \frac{ds}{U.\vec{\tau}})^2 \; &+ (\textstyle\int_{\Gamma_i} \|\frac{\partial \vec{n}}{\partial s}\| - \int_{\Gamma_i^0} \|\frac{\partial \vec{n}}{\partial s}\|)^2 \\ &+ (\textstyle\int_{\Gamma_o} \|\frac{\partial \vec{n}}{\partial s}\| - \int_{\Gamma_o^0} \|\frac{\partial \vec{n}}{\partial s}\|)^2, \end{aligned} \tag{5.2}$$

where s is the curvilinear coordinate and $(\vec{\tau}, \vec{n})$ a local orthonormal basis. The last two terms have been introduced to control wall regularity. Indeed, we noticed that losing regularity increases band dispersion. We can see that the new cost function is much more complicated, but it is suitable for incomplete sensitivity reducing the cost of gradient calculation.

Finally, to reduce the dependency on the state, we express the velocity along the wall using Eq. (**??**). Hence, we rewrite the first term as:

$$(\int_{\Gamma_i} \frac{-\mu ds}{\epsilon_0 \epsilon_r \zeta(\vec{\tau}.\vec{E})} - \int_{\Gamma_o} \frac{-\mu ds}{\epsilon_0 \epsilon_r \zeta(\vec{\tau}.\vec{E})})^2, \tag{5.3}$$

where ζ dependence on the concentration field of species is neglected for sensitivity evaluation.

6. Application to microfluidic devices

The control and design problem we consider concerns a microfluidic electrophoretic separation device. In these devices a very narrow sample plug is electroosmotically extracted from the sample reservoir into the separation channel. Then an axial electric field is applied in the separation channel and the various ionic species in the sample plug separate according to their electrophoretic mobilities. The resolution, defined as the ratio of distance between two nearby sample peaks to the characteristic standard deviation, can be enhanced by increasing the separation channel length. However the total channel length is limited by the device area. Therefore, to maximize the channel length per unit

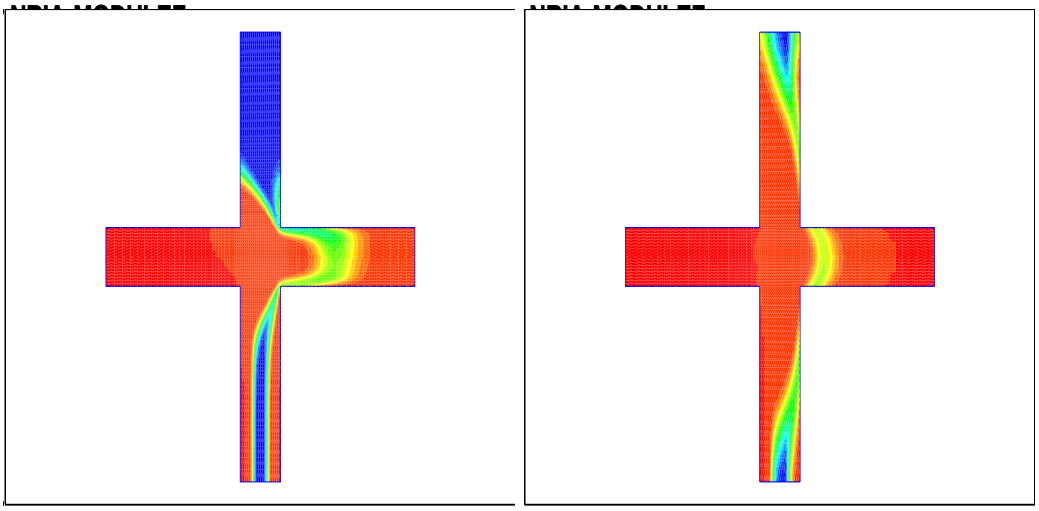

FIGURE 3. Extraction algorithm. Left: extracted band without control through the external field. Right: with control, the band dispersion has been reduced.

device area, 180 degree channel turns are incorporated. These turns permit more compact designs. However, these turns also cause sample plug dispersion, for two reasons. First, species near the inner curve travel a shorter distance and secondly, there is an electric field gradient normal to the channel, highest near the inner radius. Thus species near the inner radius travel faster than those near the outer radius. The total sample plug variance is governed by both the injected sample plug and dispersion induced by the turns. For high resolution separations it is essential to reduce and control the sample plug skew and dispersion (Probstein 1995; Culbertson *et al.* 1998 and Molho *et al.* 2001).

The problem of minimization of the dispersion of the initial extracted sample plug is solved by tuning the external electric field in a cross geometry. Once the plug is injected it is convected, and the aim is to design the optimum 180 turns to minimize the skew and dispersion. Indeed, the skew and dispersion are due only to changes in the curvature of the channel. The control parameterization is therefore based, for shape optimization, on a geometrical CAD-free model (Mohammadi 1997) and for the initial control problem on the externally applied electric field. Hence in the first case the size n of the control space is large, while it is small in the second case.

7. Concluding Remarks

The main ingredients of our minimal-complexity control and optimization platform are incomplete sensitivity evaluation and dynamic minimization algorithms. The minimal complexity has to be understood in the sense that design or control have the same cost as the solution of the direct problem. We have successfully applied these ideas to design and control microfluidic devices to reduce sample plug dispersion and skew. Current efforts concern the extension of the present approach to optimize sample stacking. Sample stacking is an extensively used technique in biochemical analysis for enhancing the concentration to detect trace-level sample constituents.

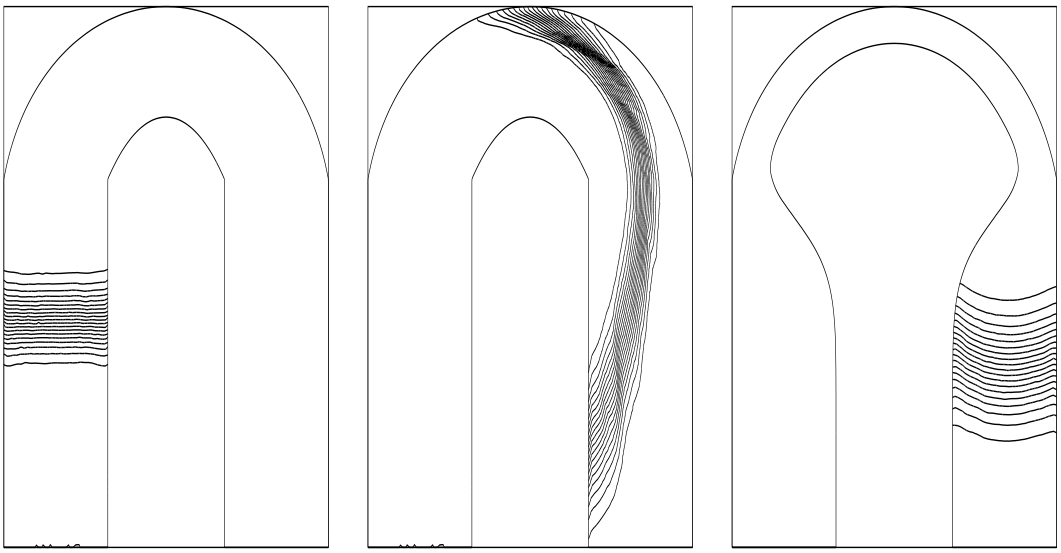

FIGURE 4. Design of 180 degree turns minimizing the band skew. Left: the original turn. Right: optimized. The initial band geometry is almost conserved enabling high resolution electrophoretic separations.

REFERENCES

ATTOUCH, H. & COMINETTI, R. 1996 A dynamical approach to convex minimization coupling approximation with the steepest descent method. *J. Diff. Equations* **128**, 519-540, 1996.

CABOT, A. 2001 Etude mathématiques de systèmes dynamiques pour minimisation globale. PhD Thesis, University of Montpellier.

CULBESTON, C. T., JACOBSON, S. C. & RAMSEY, J. 1998 Dispersion sources for compact geometries on microchips. *Analytical Chem.* **70**, 3781-3789.

MOHAMMADI, B. 1997 Practical applications to fluid flows of automatic differentiation for design problems. *Von Karman Institute* Lecture Series 1997-05.

MOHAMMADI, B. 1999a Flow control and shape optimization in aeroelastic configurations. *AIAA* paper 99-0182.

MOHAMMADI, B. 1999b Dynamical approaches and incomplete gradients for shape optimization and flow control. *AIAA* paper 99-3374.

MOHAMMADI, B. & PIRONNEAU, O. 2001 *Applied Shape Design for Fluids*, Oxford Univ. Press.

MOHAMMADI, B. & J. SANTIAGO, J. 2001 Simulation and design of extraction and separation fluidic devices. *M2AN* **35**, 513-523

MOLHO, J., HERR, A., SANTIAGO, J., KENNY, T. BRENNEN, R., GORDON, G., & MOHAMMADI, B. 2001 Optimization of turn geometries for on-chip electrophoresis. *Analytical Chem.* **73**, 1350-1360.

PROBSTEIN R.F. 1995 *Physicochemical Hydrodynamics*, Wiley.